

Figure 2. Schematic illustration which shows the formation of a diastereomeric pair by inclusion. R and S denote the stereochemical configuration of induced chiral center, and D-(+) denotes the configuration of naturally occurring β -cyclodextrin.

proton ENDOR spectra from the β -hydrogen are obtained as a doublet (Figure 1B). The hfs was analyzed to be 0.274 and 0.311 mT. In contrast proton-ENDOR spectra of the "tert-butyl-in" inclusion complex gives only a single line with an hfs of 0.465 mT. Nitrogen-ENDOR peaks were not observed under these conditions because the optimum temperature for the N-ENDOR line is expected to be higher than room temperature, and at these temperatures the equilibrium favors the free species. Also the proton-ENDOR spectrum of the free nitroxide **1** cannot be obtained at room temperature. Inclusion in cyclodextrin provides just enough restriction in tumbling motion for **1** so that an ENDOR signal can be obtained at the same temperature as used for the ESR experiments. Hfs constants obtained by ENDOR and ESR are listed in Table I.

The doublet structure near 18.5 MHz of the proton-ENDOR line of the "phenyl-in" inclusion complex is interpreted in terms of the formation of a diastereomeric mixture. The inclusion of one phenyl group in **1** changes the α -carbon into an asymmetric carbon. Since the β -cyclodextrin used is the D-(+) optical isomer, the combination with a newly formed chiral center in the spin probe can produce a diastereomeric mixture. The different configurations in the probe produced by β -cyclodextrin are schematically illustrated in Figure 2.

The inclusion of the phenyl group by either the narrow or wide end of β -cyclodextrin could give two different complexes. However, space filling models show that the inner diameter of the narrower end of β -cyclodextrin is approximately 4.5 Å which should not be wide enough to include either the phenyl group or the tert-butyl group.

The difference in hfs of diastereomeric nitroxides in which two asymmetric carbons exist on one side of the nitroxide function has been extensively studied.¹⁰⁻¹² The difference in β -hydrogen hfs in such cases is usually 0.07 to 0.09 mT compared to 0.04 mT for the present example. An estimation of the dihedral angle difference by the Heller-McConnell equation¹³ gives 0.5°. Although the NMR spectrum of a solute-solvent diastereomeric pair is widely used¹⁴ for the determination of optical purity, such examples in ESR spectroscopy are not common. Recently however, Stegmann et al.¹⁵ observed a splitting of the proton-ENDOR line of a chiral phenoxyl radical in an optically active solvent. The formation of a solute-solvent diastereomeric pair is responsible for this separation, and the difference in the β -hydrogen hfs is again very small (0.03 mT). The interaction responsible for this separation is of the same type as in the present case.

Cyclodextrin solutions of **1** were prepared by the method described previously.⁹ The solutions were investigated in a quartz flat cell, 5 mm wide and 0.3 mm inside diameter. ESR and

ENDOR spectra were obtained by using a Bruker ER200D-SRC spectrometer with ENDOR accessory. Temperature was controlled with chilled nitrogen gas with a Bruker VT4100 variable temperature unit. The spectrometer settings were specified in the figure captions.

Acknowledgment. Funding of the purchase of the ENDOR spectrometer and support for ongoing research by the Natural Sciences and Engineering Research Council of Canada is gratefully acknowledged.

The Resonance Raman Spectrum of Horseradish Peroxidase Compound I

Ki-Jung Paeng and James R. Kincaid*

Chemistry Department, Marquette University
Milwaukee, Wisconsin 53233

Received March 21, 1988

The oxidation of substrates by horseradish peroxidase proceeds via the formation of two key intermediates. Upon reaction with H_2O_2 , the active site (histidyl imidazole ligated protoheme) undergoes a two-electron oxidation to form compound I (HRP-I), generally formulated as a ferryl (porphyrin π -cation radical). A subsequent one-electron reduction by substrate yields a ferrylporphyrin species, compound II (HRP-II).¹ The initially formed species (HRP-I) is but one example of what is believed to be a common intermediate in the enzymatic cycles of several important oxidative heme enzymes.² Thus, characterization of the structure and reactivity of these species is of intense current interest.¹⁻³

Resonance Raman spectroscopy,⁴ well-suited to the investigation of the active site structure of heme proteins and reactive intermediates, has been successfully applied to the study of the resting state⁵ and the (ferrylporphyrin) HRP-II species.⁶ Unfortunately, the inherent reactivity and photolability¹ of HRP-I have prevented unambiguous documentation of its RR spectrum. An early report of this spectrum^{7a} was later shown to be attributable to a photogenerated mixture of the ferrous and HRP-II species.^{7b} More recently, efforts were made to eliminate these problems by using relatively low (CW) laser powers with flowing samples⁸ or short duration (10 ns) laser pulses.⁹ However, the frequencies reported for HRP-I in these studies are apparently anomalous by comparison with the RR data obtained for metalloporphyrin π -cation radicals by Babcock's group^{10,11} and ourselves.¹² Specifically,

(1) (a) Dunford, H. B.; Stillman, J. S. *Coord. Chem. Rev.* **1976**, *19*, 187-251. (b) Yamazaki, I.; Tamura, M.; Nakajima, R. *Mol. Cell. Biochem.* **1981**, *40*, 143-153.

(2) (a) *Cytochrome P-450, Structure, Mechanisms and Biochemistry*; Ortiz de Montellano, P. R., Ed.; Plenum: New York, 1986. (b) Burdvig, G. W.; Stevens, T. H.; Chan, S. I. *Biochemistry* **1980**, *19*, 5275-5285; **1981**, *20*, 3912-3921.

(3) Frew, J. E.; Jones, P. In *Advances in Inorganic and Bioinorganic Mechanism*; Academic Press: New York, 1984; Vol. 3, 175-215.

(4) Spiro, T. G. In *Iron Porphyrins*; Lever, A. B. P., Gray, H. E., Eds.; Addison-Wesley: Reading, MA, 1983; part 2, 89-160.

(5) (a) Loehr, T. M.; Loehr, J. S. *Biochim. Biophys. Res. Commun.* **1973**, *55*, 218-223. (b) Rakshit, G.; Spiro, T. G. *Biochemistry* **1974**, *13*, 5317-5323. (c) Teraoka, J.; Kitagawa, T. *J. Biol. Chem.* **1981**, *256*, 3969-3977.

(6) (a) Terner, J.; Sitter, A. J.; Reczek, C. M. *Biochim. Biophys. Acta* **1985**, *828*, 73-80. (b) Hashimoto, S.; Tatsumo, Y.; Kitagawa, T. *Proc. Natl. Acad. Sci. U.S.A.* **1986**, *83*, 2417-2421.

(7) (a) Teraoka, J.; Ogura, T.; Kitagawa, T. *J. Am. Chem. Soc.* **1982**, *104*, 7354-7356. (b) Van Wart, H. E.; Zimmer, J. *J. Am. Chem. Soc.* **1985**, *107*, 3379-3381.

(8) Ogura, T.; Kitagawa, T. *J. Am. Chem. Soc.* **1987**, *109*, 2177-2179.

(9) (a) Oertling, W. A.; Babcock, G. T. *J. Am. Chem. Soc.* **1985**, *107*, 6406-6407. (b) Oertling, W. A.; Babcock, G. T. *Biochemistry* **1988**, in press.

(10) Oertling, W. A.; Salehi, A.; Chung, Y. C.; Leroy, G. E.; Chang, C. K.; Babcock, G. T. *J. Phys. Chem.* **1987**, *91*, 5887-5898.

(10) Kotake, Y.; Kuwata, K.; Janzen, E. G. *J. Phys. Chem.* **1979**, *83*, 3024.

(11) Kotake, Y.; Kuwata, K. *Bull. Chem. Soc. Jpn.* **1981**, *54*, 394.

(12) Kotake, Y.; Kuwata, K. *Can. J. Chem.* **1982**, *60*, 1610.

(13) Heller, C.; McConnell, H. M. *J. Chem. Phys.* **1960**, *32*, 1535.

(14) For example, see: Pirkle, W. H.; Pochapsky, T. C. *J. Am. Chem. Soc.* **1986**, *108*, 5627.

(15) Stegmann, H. B.; Wendel, H.; Dao-Ba, H.; Schuler, P.; Scheffer, K. *Angew. Chem., Int. Ed. Engl.* **1986**, *25*, 1007.

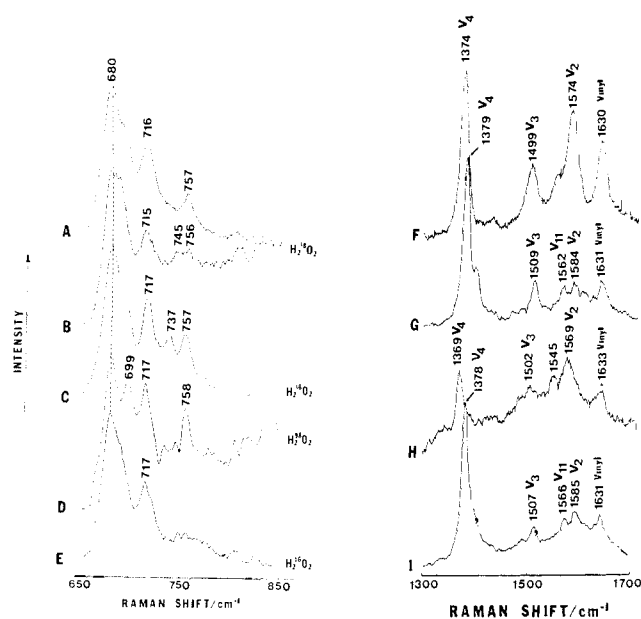


Figure 1. Resonance Raman spectra of horseradish peroxidase and enzymatic intermediates: A. resting state HRP, pH 8.4, low frequency; B. HRP-II, low frequency, pH 8.4, oxidation with $\text{H}_2^{18}\text{O}_2$; C. HRP-I, low frequency, pH 7.0, oxidation with $\text{H}_2^{16}\text{O}_2$; D. HRP-I, low frequency, pH 7.0, oxidation with $\text{H}_2^{18}\text{O}_2$; E. HRP-I, low frequency, pH 7.0, oxidation with $\text{H}_2^{16}\text{O}_2$, high laser power; F. resting state HRP, pH 7.0, high frequency; G. HRP-II, pH 7.0, high frequency; H. HRP-I, pH 7.0, high frequency; I. HRP-I, pH 7.0, high frequency, high laser power. Conditions: The HRP-I spectra were obtained as described in the text. The resting state and HRP-II spectra were obtained in spinning cells as described in ref. 6a. The 406.7-nm line from a Coherent Model 100-K3 was employed for excitation (10–50 mW at the sample). The total acquisition time for spectra A, B, F, and G was 100 s, while that for spectra C, D, E, H, and I was 40 s.

upon cation radical formation the following behavior is expected:¹³ ν_4 downshifts by 5–15 cm^{-1} ; ν_3 shifts only slightly downward by 2–8 cm^{-1} ; and ν_2 shifts up by $\sim 20 \text{ cm}^{-1}$ for a_{1u} species but shows a substantial downshift (20–30 cm^{-1}) for a_{2u} species. The accepted a_{2u} formulation of HRP-I¹ leads to the expectation of significant downshifts in ν_2 and ν_4 and a slight downshift in ν_3 relative to their values in the spectrum of HRP-II. Insignificant shifts in these key features relative to their values for HRP-II were observed in the previously reported spectra of HRP-I.^{8,9} In the most recent work,^{9b} the lack of such shifts was noted and interpreted as evidence of either photolability or extensive delocalization of the spin density onto the axial ligands. Here, we report the results of our recent efforts to observe the RR spectrum of HRP-I and point out that the frequencies observed for the characteristic heme core modes are consistent with the results of the model π -cation studies. More importantly, we have observed, for the first time, a feature which is attributable to the $\nu(\text{Fe}-\text{O})$ of the oxyferryl fragment of this apparently ubiquitous intermediate.

In our experiments, a flowing solution of HRP¹⁴ was mixed with a flowing buffer solution containing a 2-fold to 5-fold excess of H_2O_2 . The mixed solution flows through a length of polyethylene tubing to a device¹⁶ which generates a high velocity stream of droplets ($\sim 100 \mu\text{m}$ diameter) which then passes through the focussed laser beam.¹⁷ The scattered light is focussed onto the

slits of a Spex Model 1877A spectrometer equipped with a Tracor-Northern Model 6500 photodiode array detection system. The electronic spectrum of the collected stream (obtained within a few minutes) closely corresponded to that published for HRP-I.¹

In Figure 1 are shown the RR spectra of the resting state HRP (traces A and F), HRP-II (traces B and G), and the spectrum of the green reaction product obtained as described above (traces C, D, and H).¹⁸ The spectra of the first two species are essentially identical with those published previously.^{5,6} The spectrum shown in H exhibits a relatively strong feature at 1369 cm^{-1} which is readily assigned to the "oxidation state marker band", ν_4 , with conventional nomenclature.⁴ While bands between 1500 and 1600 cm^{-1} are difficult to distinguish with the relatively low resolution attainable with this spectroscopic system, features which can be attributed to ν_3 and ν_2 are observed at 1502 and 1569 cm^{-1} ,¹⁹ yielding downshifts (relative to HRP-II) in agreement with expectations based on the model compound work;¹² i.e., $\Delta\nu_3 = -15$, $\Delta\nu_2 = -7$, and $\Delta\nu_4 = -10 \text{ cm}^{-1}$. We emphasize that this is the first reported spectrum of HRP-I which exhibits the expected core marker frequencies and that it is not likely that of a photoproduct.²⁰

The identification of the spectrum in trace H as that of HRP-I requires support through the observation of feature which can be attributed to $\nu(\text{Fe}-\text{O})$ of the oxyferryl fragment. In order to locate this feature we have conducted studies with $\text{H}_2^{18}\text{O}_2$. As can be seen in trace C, a weak feature is observed at 737 cm^{-1} which essentially disappears and is replaced by a new band at 699 cm^{-1} when $\text{H}_2^{18}\text{O}_2$ is employed (trace D).²¹ We emphasize that in many experiments (~ 30) the 737- cm^{-1} feature is always observed when using $\text{H}_2^{16}\text{O}_2$, while the 699 cm^{-1} is *never* observed. Conversely, the 699- cm^{-1} feature is *always* observed when using $\text{H}_2^{18}\text{O}_2$ as the oxidant (eight experiments).

Bajdor and Nakamoto²² first observed $\nu(\text{Fe}-\text{O})$ at 852 cm^{-1} for a matrix isolated ferrylporphyrin (nonradical). Subsequent work by Terner et al.^{6a} and Kitagawa and co-workers^{6b} identified $\nu(\text{Fe}-\text{O})$ at ~ 790 and 776 cm^{-1} for HRP-II (at high and low pH, respectively). Our identification of $\nu(\text{Fe}-\text{O})$ at 737 cm^{-1} for HRP-I represents a (776–737) 39- cm^{-1} downshift upon radical formation and implies a substantial weakening of the Fe–O linkage. While the magnitude of this shift is surprisingly large, we wish to point out that it is entirely consistent with model compound studies as discussed below.

The $\nu(\text{Fe}-\text{O})$ of the (nonradical) ferryltetramesitylporphine (OFeTMP) has been observed at 843 cm^{-1} in toluene solutions.²³ Recently, we have studied the RR spectrum of the ferryltetramesitylporphine π -cation [$\text{OFe}(\text{TMP}^+)^+$] and have identified the oxygen isotope sensitive $\nu(\text{Fe}-\text{O})$ at 802 cm^{-1} .²⁴ Thus, the shift observed in the model compound systems essentially matches that observed for the proteins. Apparently, all other factors being held constant, oxidation of the macrocycle induces a $\sim 40\text{-cm}^{-1}$

(17) The emerging stream of droplets has a linear velocity of $\sim 20 \text{ m/s}$ which corresponds to a well-defined 3- μs residence time in the CW laser beam. The previously reported study of flowing solutions yielded a sample residence time in the beam of 5 ms.⁸ We also note that in our experiments the time lapse between initial mixing of the two solutions and droplet generation (and thus Raman detection) is typically 10–50 s.

(18) We wish to point out that the absolute intensities of the features in the HRP-I spectrum are much weaker than those of the resting state and HRP-II, in agreement with expectations based on the model compound studies.^{10–12}

(19) The 1633- cm^{-1} feature is a polarized vinyl mode and does not correspond to ν_{10} .

(20) Briefly, the spectrum shown in trace C and H are converted to a different spectrum (traces E and I) at higher laser powers ($>100 \text{ mW}$). Further studies of this photolysis reaction under various solution conditions and with different residence times and laser powers are planned.

(21) The apparent isotopic shift (38 cm^{-1}) is similar to those observed for HRP-II (ref 6b) and the photoproduct of HRP-I.^{9b}

(22) Bajdor, K.; Nakamoto, K. *J. Am. Chem. Soc.* **1984**, *106*, 3045–3046.

(23) (a) Hasimoto, S.; Tatsumo, Y.; Kitagawa, T. *Proceedings of the Tenth International Conference on Raman Spectroscopy*; Peticolas, W. L., Hudson, B., Eds.; University of Oregon: Eugene, OR, 1986; pp 1–28. (b) Paeng, I. R.; Shiwaku, H.; Nakamoto, K. *J. Am. Chem. Soc.* **1988**, *110*, 1995–1996.

(24) Kincaid, J. R.; Schneider, A. J.; Paeng, K.-J., submitted for publication.

(11) Salehi, A.; Oertling, W. A.; Babcock, G. T.; Chang, C. K. *Inorg. Chem.* **1987**, *26*, 4296–4298.

(12) Czernuszewicz, R. S.; Macor, K. A.; Li, X.-Y.; Kincaid, J. R.; Spiro, T. G., submitted for publication.

(13) On the basis of our most recent studies.¹² The nomenclature used for mode identification (i.e., ν_2 , ν_3 , etc.) corresponds to that commonly accepted.⁴

(14) HRP (type II) was obtained from Sigma Chemical Co. and the band C isoforms isolated as previously described.¹⁵ The solution of HRP was $1 \times 10^{-4} \text{ M}$ in $5 \times 10^{-2} \text{ M}$ phosphate buffer, pH 7.0.

(15) Shannon, L. M.; Kay, E.; Lew, J. Y. *J. Biol. Chem.* **1966**, *241*, 2166–2172.

(16) Simpson, S. F.; Kincaid, J. R.; Holler, F. J. *Anal. Chem.* **1986**, *58*, 3163–3166.

downshift of $\nu(\text{Fe}-\text{O})$ of the oxyferryl fragment. It should be noted that Spiro and co-workers²⁵ have recently observed an *upshift* of $\nu(\text{V}-\text{O})$ of vanadyl octaethylporphyrin [OV(OEP)] upon formation of [OV(OEP*)⁺]. This complex forms an "a_{1u}-like" radical while HRP-I and [OFe(TMP*)⁺] are best characterized as "a_{2u}-like".^{12,26} While further studies will be needed to evaluate this issue, the weakening of Fe-O in "a_{2u}-like" and strengthening in "a_{1u}-like" radicals may prove to hold generally. Thus, the inherent reactivity of the Fe-O fragment in the enzyme systems may be indirectly controlled by any steric and environmental factors which affect the orbital character of the metalloporphyrin radical fragment.

Acknowledgment. We gratefully acknowledge support of this work from the National Institutes of Health (DK-35153). The Raman spectroscopic equipment used in this work was partially funded by a grant from the National Science Foundation (CHE-8413956). We thank Professor G. Babcock (Michigan State University) for providing a copy of his manuscript prior to publication.

(25) Oliver Su, Y.; Czernuszewicz, R. S.; Miller, L. A.; Spiro, T. G. *J. Am. Chem. Soc.* **1988**, *110*, 4150-4157.

(26) Browett, W. R.; Gasyňa, Z.; Stillman, M. J. *J. Am. Chem. Soc.* **1988**, *110*, 3633-3640.

Activation of Methane by the Reactive Intermediate Tris(trimethylphosphine)osmium(0)

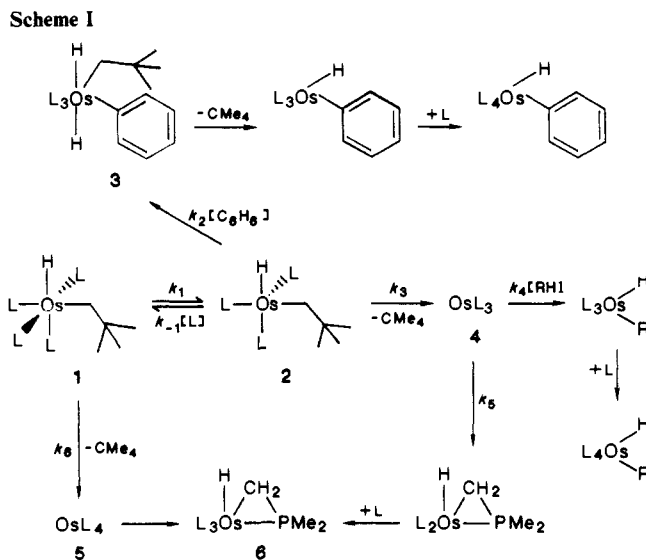
T. Gregory P. Harper, Ronald S. Shinomoto,
Mark A. Deming, and Thomas C. Flood*

Department of Chemistry
University of Southern California University Park
Los Angeles, California 90089-0744

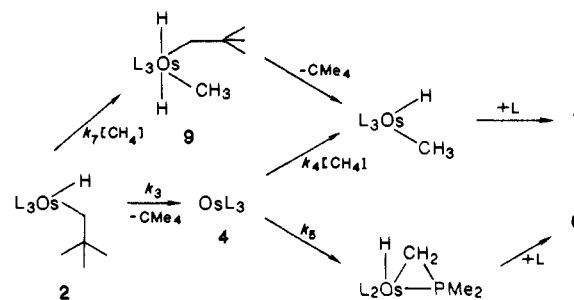
Received August 15, 1988

The activation of hydrocarbon C-H bonds by soluble metal complexes has been a significant goal of organometallic chemists for two decades. In the past few years substantial progress has been made.^{1,2} We have recently described the mild intermolecular activation of carbon-hydrogen bonds in benzene by intermediates generated in the thermolysis of *cis*-L₃Os(H)(CH₂CM₂), L = P(CH₃)₃, **1**.³ We have also studied the activation of C-H bonds in SiMe₄, in the benzylic position of mesitylene, and intramolecularly in L.^{4,5} A summary of the essential features of our conclusions is shown in Scheme I.

While the intermediate L₃Os (**4**) is intercepted by SiMe₄ to afford *cis*-L₄Os(H)(CH₂SiMe₃), **8**, and by mesitylene to give only benzylic C-H activation, it does not afford an isolable alkyl hydride complex from reaction with any alkane solvent that we have used, including pentane, cyclopentane, hexane, cyclohexane, and octane. We have previously concluded that both dissociation of L from **1**³ (path 1)⁶ and neopentane reductive elimination from **1**³⁻⁵ (path



Scheme II



6) are driven by the steric crowding in **1**. It is possible that even L₃Os is subject to some steric inhibition of reaction with alkanes; hence, the smallest alkane, methane, might have the greatest chance of competing with cyclometalation (path 5) to give C-H activation via path 4. We report here that methane is activated by L₃Os, albeit in low yield, affording **7**. This is one of the first examples of observation of a non-cyclopentadienyl-containing methyl hydride complex from reaction of a soluble complex with methane.⁷

Pyrolysis of **1** in cycloalkane solvent at 80 °C under methane gas at pressures sufficient to give up to ca. 2 M solutions results in formation of a mixture of cyclometalation product **6** and methylhydride **7** as the only significant products with the latter in yields up to ca. 16%.⁸ The ³¹P NMR resonances of **7** are never observed in thermolyses of **1** when methane is absent, and use of ¹³C-CH₄ yielded (methyl-¹³C)-**7**.

Methane activation could reasonably proceed by reaction with L₃Os⁰, **4**, (path 4), L₃Os(H)Np, **2**, (path 7, Scheme II), or L₄Os⁰, **5**. Reaction with **5** can be ruled out as follows. We have previously measured k_1 to be $7.3 \times 10^{-4} \text{ s}^{-1}$, at least 200 times faster than k_{obsd} , so some subsequent step is rate-determining. A plot of k_{obsd} vs $1/[\text{L}]$ affords a line with slope $(k_1 k_3 / k_{-1})$ of 2.7×10^{-9} and an intercept (k_6) of 1.1×10^{-6} . Thus, with excess added L (0.16 M), only the L-independent path 6 functions, and we observe that this path leads only to **6**; no **7** is formed.

Distinguishing between paths 4 and 7 is more difficult. The overall rate of reaction proceeding via path 7 should be dependent

(6) Each reaction path in Scheme I will be referred to in the text by the numerical subscript of the rate constant for that path.

(7) The only other example known to us is that of ref 2h wherein methane is activated by an intermediate in the thermolysis of [bis(dicyclohexylphosphino)ethane](hydrido)neopentylplatinum(II). This intermediate is proposed to be [bis(dicyclohexylphosphino)ethane]platinum(0).

(8) Pyrolyses were carried out in sealed, thick-walled NMR tubes under 40-65 atm of methane pressure heated by total immersion in an oil bath at 80 °C. Product analysis and kinetics measurements were easily made by following the characteristic ³¹P NMR resonances of components of the reactions, all of which are known.³

(1) For leading references outlining the development of this subject, see: Crabtree, R. H.; *Chem. Rev.* **1985**, *85*, 245-269.

(2) For examples specifically of activation of methane by soluble metal complexes, see: (a) Shilov, A. E.; Shteinman, A. A. *Coord. Chem. Rev.* **1977**, *24*, 97. (b) Watson, P. L. *J. Am. Chem. Soc.* **1983**, *105*, 6491-6493. (c) Hoyano, J. K.; McMaster, A. D.; Graham, W. A. G. *Ibid.* 7190-7191. (d) Wax, M. J.; Stryker, J. M.; Buchanan, J. M.; Kovac, C. A.; Bergman, R. G. *Ibid.* **1984**, *106*, 1121-1122. (e) Fendrick, C. M.; Marks, T. J. *Ibid.* 2214-2216. (f) Wenzel, T. T.; Bergman, R. G. *Ibid.* **1986**, *108*, 4856-4867. (g) Thompson, M. E.; Baxter, S. M.; Bulls, A. R.; Burger, B. J.; Nolan, M. C.; Santarsiero, B. D.; Schaefer, W. P.; Bercaw, J. E. *Ibid.* **1987**, *109*, 203-219. (h) Hackett, M.; Whitesides, G. M. *Ibid.* **1988**, *110*, 1449-1462.

(3) Desrosiers, P. J.; Shinomoto, R. S.; Flood, T. C. *J. Am. Chem. Soc.* **1986**, *108*, 7964-7970.

(4) Part of the work outlined in Scheme I has been the subject of a communication: Desrosiers, P. J.; Flood, T. C. *J. Am. Chem. Soc.* **1986**, *108*, 1346-1347. The activation of SiMe₄ and the phosphine-dependent intramolecular activation of PMe₃ were suggested in this communication to proceed via Os(IV) intermediates. However, more extensive new data clearly point to the presence of path 3. These data will be presented in detail.⁵

(5) Desrosiers, P. J.; Shinomoto, R. S.; Harper, T. G. P.; Deming, M. A.; Flood, T. C., manuscript in preparation.